

Cationic Nanoparticles Stabilize Zwitterionic Liposomes Better than Anionic Ones

Yan Yu, Stephen M. Anthony, Liangfang Zhang, Sung Chul Bae, and Steve Granick*

Departments of Materials Science and Engineering, Chemistry, and Physics, University of Illinois, Urbana, Illinois 61801

Received: April 5, 2007

Building upon the finding that zwitterionic liposomes can be stabilized against fusion up to very high surface coverage by the adsorption to submonolayer ($\approx 25\%$) surface coverage of nanoparticles (Zhang, L.; Granick, S. *Nano Lett.* **2006**, *6*, 694), here we compare the efficacy of cationic and anionic nanoparticles for the stabilization of DLPC, 1,2-dilauroyl-*sn*-glycero-3-phosphocholine. This is rationalized by considering that because the phospholipid zwitterionic headgroup terminates with positive charge, lipids beneath an adsorbed nanoparticle bind more weakly when the nanoparticle charge is cationic. Going beyond the earlier qualitative study, here single-particle tracking using epi-fluorescence imaging is used to quantify the mobility of individual liposomes. The distribution of diffusion coefficients between different liposomes in the sample is quantified. In contrast to the colloid behavior of traditional monodisperse hard-sphere colloids, these soft, flexible, colloidal-sized objects remain fluid at 50% volume fraction of liposomes.

Introduction

Recent experiments show that submicrometer-sized phospholipid vesicles (also called liposomes) fail to fuse with one another when coated with adsorbed nanoparticles at surface coverages on the order of 25%.¹ This route to stabilization is appealing because the low occupied surface area enables these liposomes to retain the potential to react functionally with their environment. However, the original study¹ addressed only the influence of anionic nanoparticles whose charge density was high. Moreover, those studies of shelf life, at dense concentrations, were only qualitative—leaving open the question of the respective efficacy of nanoparticles of different electric charge, as well as the question whether liposomes retain fluidity, using this stabilization route, up to dense concentrations.

It is known that the P^-N^+ (phosphorus–nitrogen) dipole in zwitterionic phosphatidylcholine (PC) is nearly parallel to the local bilayer plane with an average angle of 0° to $\sim 3^\circ$ in the fluid phase.^{2–4} When this zwitterionic headgroup is exposed to an anionic nanoparticle, a simple electrostatic argument suggests tight electrostatic binding by raising the headgroup's tilt angle, because an anionic adsorbate has opposite charge as the P^- end group. Conversely, if the headgroup is exposed to a cationic nanoparticle, this is not encouraged electrostatically. The geometrical relation between the P^-N^+ dipole of the headgroup and the charge of the adsorbing nanoparticle, therefore, determines the strength of binding: anionic nanoparticles would adsorb more strongly than cationic ones. This situation is depicted schematically in the inset of Figure 1A.

We are unaware of any theoretical predictions regarding the effect on liposome stability, though our original publication on this topic attributed stabilization to the combined influences of electrostatic repulsion between adsorbed nanoparticles and steric impediments analogous to particle-stabilized emulsions.¹ Also, this is potentially analogous to a related problem, the stabilization of micrometer-sized solid particles suspended in aqueous media.⁵ Computer simulations have made the paradoxical

prediction that nanoparticles stabilize most effectively when they adsorb weakly—the reason being that in this case they are less apt to bridge between adjacent particles, less likely to tie them together.^{6–8} Here we confirm the validity of the analogy as it applies to liposomes comprised of zwitterionic lipids.

Early stages of this study, using fluorescence tagging described below, validated the hypothesis that weaker binding, rather than tight binding of nanoparticles to liposomes, was more effective. At volume fractions $\Phi > 0.50$, liposome samples bearing anionic nanoparticles formed a dense lipid phase in which individual liposomes failed to move—but liposome samples bearing cationic nanoparticles remained fluid. In the remainder of this article, we go beyond this qualitative observation and use single-particle tracking to quantify the fluidity. The volume fraction was fixed at $\Phi = 0.50$.

Materials and Methods

For study, phospholipid DLPC, 1,2-dilauroyl-*sn*-glycero-3-phosphocholine, was selected because its gel-to-fluid phase transition of -1°C was far below the experimental temperature, 23°C . The fluorescent lipid was DMPE, 1,2-dimyristoyl-*sn*-glycero-3-phosphoethanolamine, with polar head group labeled by rhodamine B (DMPE–RhB). Both lipids were obtained from Avanti Polar Lipids, Inc. Positively charged aliphatic amidine polystyrene (PS) latex, with charge density quoted by the manufacturer of 5.6 nm^2 per unit charge, and negatively charged carboxyl modified PS latex¹ were purchased from Interfacial Dynamics Corp (Eugene, OR).

Single-liposome detection of fluidity was performed in a home-built epi-fluorescence setup described elsewhere.¹ The diffusion of liposomes was tracked, using a modified implementation of standard single-particle tracking algorithms described previously, with spatial resolution of 50 nm .^{9,10} The methods of fluorescence correlation spectroscopy (FCS) were described previously.¹

Results and Discussion

We prepared large unilamellar lipid vesicles (liposomes) with a maximum diameter of 200 nm in deionized water (Millipore)

* Corresponding author. E-mail: sgranick@uiuc.edu.

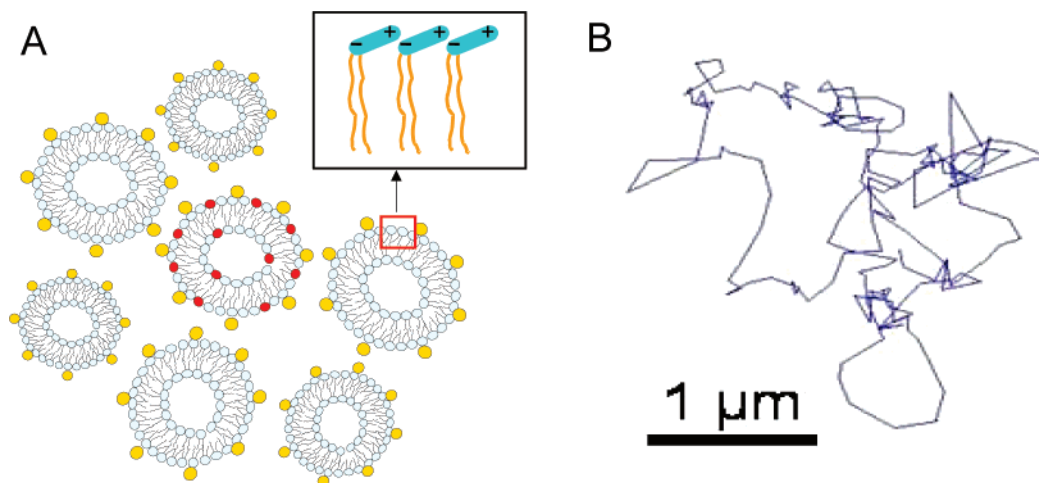


Figure 1. (A) Schematic illustration that in concentrated suspensions, DLPC liposomes with a maximum diameter of 200 nm were stabilized by nanoparticles with a diameter of 20 nm. The inset shows a schematic diagram of the P^-N^+ dipolar headgroup of a zwitterionic lipid. Therefore, an anionic nanoparticle, with electric charge opposite to that of the outermost portion of the lipid headgroup, adsorbs more strongly than a cationic nanoparticle. (B) A typical single-liposome trajectory: the time elapsed was 50 s in a condensed liposome suspension of $\Phi = 0.50$. Each step was 50 ms long.

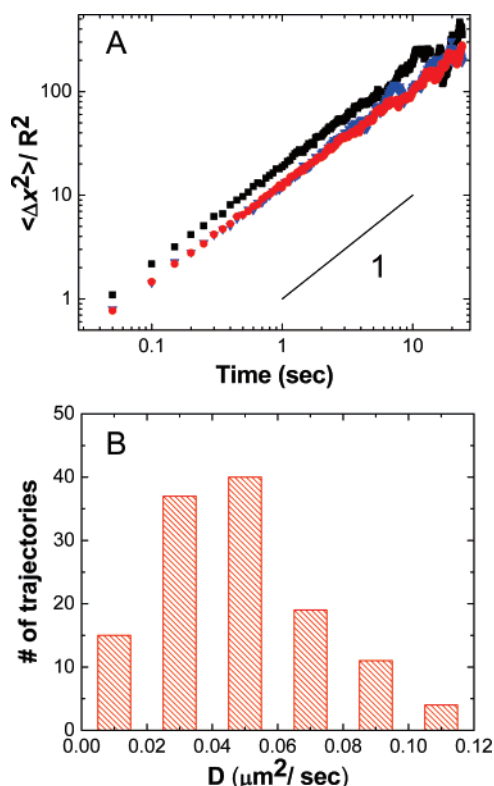


Figure 2. Diffusion of stabilized liposome at 0.50 volume fraction revealed by single-liposome tracking. (A) Mean square displacements $\langle \Delta x^2 \rangle$ in units of liposome hydrodynamic radius are plotted against time on a log–log scale for three individual liposomes. The line, a guide to the eye, has a slope of unity. (B) From the analysis of ≈ 130 trajectories, the distribution of the diffusion coefficient, determined from data of the kind illustrated in panel A, is plotted. In dilute solution, fluorescence correlation spectroscopy (FCS) showed $D \sim 0.8 \mu\text{m}^2/\text{s}$, faster by more than 1 order of magnitude.

using the well-known extrusion method, employing procedures described in detail elsewhere.¹¹ With the use of methods described elsewhere,^{1,12} liposomes of DLPC were mixed by low-power sonication with these nanoparticles, diameter 20 nm. The molar ratio of 100:1, approximately 1:1 by weight, corresponds to the upper limit of $\approx 25\%$ surface coverage if all nanoparticles adsorb. To image the liposomes, typically ≈ 500 DMPE–RhB

probes per liposome were doped into a small fraction of the liposomes, leaving the rest unlabeled and free of fluorescence. To prepare concentrated suspensions, first the liposomes were prepared at 1 vol %, then they were concentrated by bubbling nitrogen gas gently over them. To calculate the volume fraction, calculations included not only liposomes but also nanoparticles and were determined from the difference between initial and final suspension volumes. An essential point is that liposomes prepared using this method are polydisperse. Using quasi-elastic light scattering, we estimated the ratio of standard deviation to liposome diameter as 0.34. Figure 1A shows a schematic illustration.

The low concentration of fluorescent lipid—approximately 0.01% of the liposomes contained fluorescent DMPE–RhB lipid probes—enabled single-liposome detection of fluidity in a home-built epi-fluorescence setup. Parenthetically, we note that the community of scientists that studies phospholipid bilayers sometimes reserves the term “fluidity” to the 2D diffusion of lipids—our use of the term here is different, as we refer to liposome diffusion in bulk (3D) suspension.

We focused at least $2 \mu\text{m}$ away from the coverslip to avoid wall effects. Usually, the total observation time at a given focus spot was 50 s, yielding 1000 time steps of 50 ms length. Occasionally, liposomes would diffuse out of the plane of focus during this time—in these cases, those trajectories could not be used to quantify the statistics of very long trajectories, though still they were useful to quantify the statistics of shorter trajectories. These and other technical issues were discussed in an earlier publication from this laboratory.¹³ The diffusion of liposomes was tracked, using a modified implementation of standard single-particle tracking algorithms described previously, with spatial resolution of 50 nm.^{9,10} Figure 1B shows one of the representative liposome trajectories at $\Phi = 0.50$. The mean square displacement ($\langle \Delta x(t)^2 \rangle$) was linear in elapsed time—as must be so for a random walk.

From the liposome trajectories, the mean square displacements $\langle \Delta x(t)^2 \rangle = \langle (x(\tau + t) - x(\tau))^2 \rangle$ were individually computed for all trajectories that lasted longer than 100 time steps. As is frequently done for single-particle tracking,¹⁴ time averaging was employed to improve the statistics. For instance, the mean squared displacement for $\Delta t = 4$ s was calculated using the mean square of the displacements from $t = 0$ to $t = 4$ s and from $t = 4$ to $t = 8$ s. Thus, the percent uncertainty of each

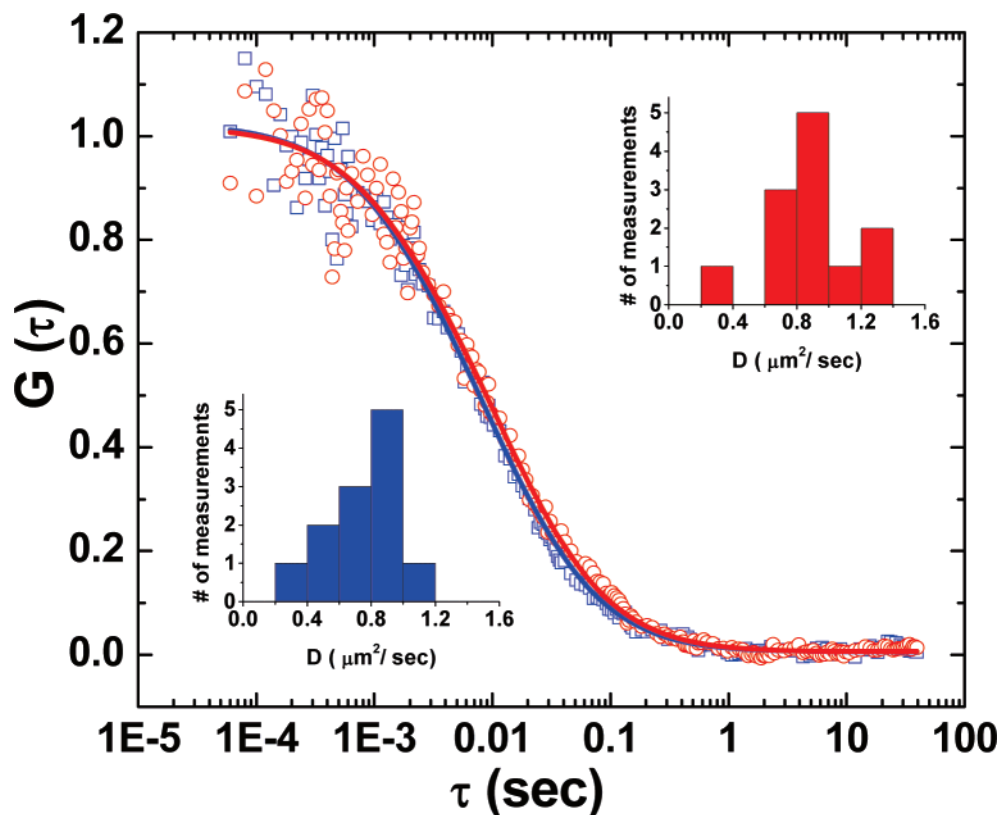


Figure 3. Fluorescence autocorrelation function $G(\tau)$ plotted as a function of logarithmic time lag τ for stabilized liposome suspensions with volume fraction $\Phi = 0.01$ before (red open circle) and after (blue open square) concentration to $\Phi = 0.50$; the data are the same within the experimental uncertainty, demonstrating lack of history dependence. The inset, comparing histograms of diffusion coefficients (D) obtained from ~ 15 measurements at volume fraction $\Phi = 0.01$ before (red) and after (blue) concentration to $\Phi = 0.50$, demonstrates that distribution around the mean of D was also unaffected.

point of the mean square displacement is approximately proportional to $t^{1/2}$. Figure 2A illustrates the mean square displacements for three individual stabilized liposomes at $\Phi = 0.50$. The displacements are in units of the liposome hydrodynamic radius. The log–log plot of individual $\langle \Delta x(t)^2 \rangle$ versus time all yielded slopes of ~ 1 , which is expected for Fickian diffusion.

Checking for dynamical heterogeneity, i.e., differences from spot to spot within the sample, diffusion coefficients $D = \langle \Delta x(t)^2 \rangle / 4t$ were calculated from individual mean square displacements. The histogram of findings is shown in Figure 2B. The uncertainty, based upon weighted linear regression, was estimated to be $0.01 \mu\text{m}^2/\text{s}$ on average. The distribution in D is attributed to polydispersity of the elementary liposomes. For comparison, for these same nanoparticle-stabilized liposomes in dilute (1%) suspension, FCS showed $D \sim 0.8 \mu\text{m}^2/\text{s}$, faster by more than 1 order of magnitude. The decrease of D at high Φ is attributed to higher solution viscosity.

Reversibility was also investigated and is illustrated in Figure 3. The same suspension was concentrated to $\Phi = 0.50$ using the procedure just described, then diluted back to $\Phi = 0.01$ by adding deionized water, and finally vesicle diffusion was remeasured using FCS using methods described previously.¹ The diffusion coefficient before and after this concentration process were unchanged.

Outlook

The capability, demonstrated in this study, to use single-particle tracking to follow the diffusion of individual liposomes within a concentrated stabilized liposome suspension offers a platform to reveal the dynamics of these flexibly shaped objects in a variety of other situations. Preliminary findings in this

laboratory show that proteins can be incorporated into the stabilized liposomes without loss of bioactivity.¹⁵

This is not the conventional use of single-particle tracking. Indeed, these findings may seem odd if one considers that conventional colloidal-sized suspensions of the type studied previously by single-particle tracking,^{16–18} monodisperse hard-sphere suspensions, undergo a freezing transition at $\Phi = 0.494$,^{17,18} which is less than the volume fraction for which liquid-like diffusion of individual liposomes has been demonstrated in this article. At least three factors may contribute to the retention of fluidity in the present liposome system: the flexible lipid bilayer membrane, the polydispersity of the liposomes, and the strong electrostatic repulsion between cationic nanoparticles.

Acknowledgment. We thank Dr. Jacinta Conrad and Dr. Angelo Cacciuto for helpful discussion, Dr. Huilin Tu for help with dynamic light scattering measurements, and Mr. Yunus Kinkhabwala for help with single-particle tracking. This work was supported by the U.S. Department of Energy, Division of Materials Science, under Award No. DEFG02-02ER46019. S.C.B. acknowledges assistance through the Water CAMPWS, a Science and Technology Center of Advanced Materials for the Purification of Water (NSF CTS-0120978) and also through NSF (NIRT) CBET 060978. S.M.A. acknowledges the NSF for financial support in the form of a graduate research fellowship.

References and Notes

- (1) Zhang, L.; Granick, S. *Nano Lett.* **2006**, *6*, 694.
- (2) Zhang, L.; Spurlin, T.; Gewirth, A. A.; Granick, S. *J. Phys. Chem. B* **2006**, *110*, 33.
- (3) Pink, D. A.; Belaya, M.; Lavadny, V.; Quinn, B. *Langmuir* **1997**, *13*, 1701.

- (4) Hauser, H.; Pascher, I.; Pearson, R. H.; Sundell, S. *Biochim. Biophys. Acta* **1981**, *650*, 21.
- (5) Tohver, V.; Smay, J. E.; Braem, A.; Braun, P.; Lewis, J. A. *Proc. Natl. Acad. Sci. U.S.A.* **2001**, *98*, 8950.
- (6) Liu, J. W.; Luijten, E. *Phys. Rev. Lett.* **2004**, *93*, 247802.
- (7) Liu, J. W.; Luijten, E. *Phys. Rev. E* **2005**, *72*, 061401.
- (8) Karanikas, S.; Louis, A. A. *Phys. Rev. Lett.* **2004**, *93*, 248303.
- (9) Crocker, J. C.; Grier, D. G. *J. Colloid Interface Sci.* **1996**, *179*, 298.
- (10) Anthony, S.; Zhang, L.; Granick, S. *Langmuir* **2006**, *22*, 5266.
- (11) Xie, A. F.; Yamada, R.; Gewirth, A. A.; Granick, S. *Phys. Rev. Lett.* **2002**, *89*, 246103.
- (12) Zhang, L.; Hong, L.; Yu, Y.; Bae, S. C.; Granick, S. *J. Am. Chem. Soc.* **2006**, *128*, 9026.
- (13) Anthony, S.; Hong, L.; Kim, M.; Granick, S. *Langmuir* **2006**, *22*, 9812.
- (14) Kasper, A.; Bartsch, E.; Sillescu, H. *Langmuir* **1998**, *14*, 5004.
- (15) Zhang, L.; Dammann, K.; Bae, S. C.; Granick, S. *Soft Matter* **2007**, *3*, 551.
- (16) Weeks, E. R.; Crocker, J. C.; Levitt, A. C.; Schofield, A.; Weitz, D. A. *Science* **2000**, *287*, 627.
- (17) Weeks, E. R.; Weitz, D. A. *Phys. Rev. Lett.* **2002**, *89*, 095704.
- (18) Kegel, W. K.; van Blaaderen, A. *Science* **2000**, *287*, 290.